Astronomical and Astrophysical Transactions (*AApTr*), 2012, Vol. 27, Issue 3, pp. 517–522,
ISSN 1055-6796, Photocopying permitted by license only, ©Cambridge Scientific Publishers

Magnetic field of protostellar accretion disks

S.N. Zamozdra[1*], A.G. Zhilkin[1,2]

[1] *Chelyabinsk State University*
[2] *Institute of Astronomy RAS*

Received 20 November, 2008

One- and two-dimensional (1D and 2D) MHD models of prestellar core collapse are presented. 1D models show that ambipolar diffusion slightly weakens magnetic field in core envelope while ohmic diffusion in the region 1–100 AU weakens the magnetic field of protostar and its vicinity by 2 orders of magnitude in comparison with frozen-in field. The region of magneto-rotational stability (dead zone) is located at 0.5–30 AU. 2D models show that all cores flatten along magnetic field, therefore it decreases by 1–2 orders of magnitude in comparison with 1D cases.

Keywords: Star formation; Collapse; Ionization fraction; Magnetic field

1 Introduction

The gravitational collapse of molecular cloud cores leads to the formation of protostars – hot ($T \simeq 1000$ K) gas balls which contract at Kelvin–Helmholtz time scale to stellar radii. Protostellar masses increase significantly due to accretion, usually from rotationally supported disks (see [1]). Several mechanisms to remove the angular momentum from the disks allow the accretion onto protostars: (a) magneto-centrifugal wind, (b) magnetic pressure driven jets, (c) turbulent viscosity and (d) gravitational torques. Mechanisms (a–c) depend on the magnetic field of protostellar accretion disks, $\vec{B}_{\rm ad}$. It is poorly known from the observations (see [2]) therefore theorists prescribe it. In the present work we calculate $\vec{B}_{\rm ad}$ as the fossil magnetic field of molecular cloud cores with the help of 1D numerical models. Initial collapse stage is investigated also with the help of 2D numerical models (Section 2). Both ambipolar and ohmic diffusions (AD and OD) as well as cosmic ray ionization and thermal ionization are considered. In Section 3 the modelling of three molecular cloud cores: W3(main), NGC 2024 and DR21 OH 1, is described and the position of dead zones in accretion disks [3] is estimated. Comparisons and conclusions are presented in Section 4.

*Email: sezam@csu.ru

2 Models

2.1 Common properties

Five-fluid (neutrals, ions, electrons, positive and negative dust grains) magnetohydrodynamics (MHD) is used to derive (see [4]) the magnetic induction equation neglecting by friction forces between the charged species. If their velocities are almost equal (the approximation of AD) the induction equation becomes

$$\frac{\partial \vec{B}}{\partial t} = \nabla \times \left(\vec{v}_p \times \vec{B} - \eta \nabla \times \vec{B} \right), \tag{1}$$

where $\eta = c^2(4\pi\sigma)^{-1}$ is the ohmic diffusivity, σ is the total electrical conductivity of the species, $\vec{v}_p$ is the velocity of charged component that is determined from the equality of friction and electromagnetic forces: $R_{pn}(\vec{v}_p - \vec{v}_n) = (4\pi)^{-1} \left(\nabla \times \vec{B} \right) \times \vec{B}$. The friction coefficient R_{pn} includes the contributions of all charged species. Neutrals velocity $\vec{v}_n$ is calculated as the mass velocity in one-fluid MHD. In both 1D and 2D models $\vec{B}$ is axially symmetric; initial velocity field is zero.

The number densities of charged species are calculated under the condition of ionization equilibrium with the help of two joint systems of algebraic equations. The first one (see [5]) describes the production of Mg^+, HCO^+ and dust grains with charges $\pm e$ by cosmic rays (CR) and radionuclides (^{26}Al and ^{60}Fe). The second one describes the production of H^+, Li^+, Na^+, Mg^+, Al^+, Si^+, K^+, Ca^+, Rb^+, Cs^+ by the thermal radiation of medium. Dust grains are considered as the recombination sites, metal desorption sites, and charge carriers. Their sizes decrease with increasing temperature. The most refractory grain component (graphite) disappears at $T =$ 2300 K.

2.2 1D model features

The spatial derivatives of η in eq. (1) are neglected. Density ρ and velocity are centrally symmetric; spherical coordinates are used. Equation (1) and electromagnetic force are averaged over semi-spheres using analytical solution for $\vec{B}(\vec{r}, t)$. Initially $T(r)$ is constant while $\rho(r)$ and $B(r)$ are calculated from the condition of hydrostatic equilibrium at the constant ratio of magnetic and thermal pressures. The model [6] is used to obtain a piecewise power law approximation for $T(\rho)$. MHD equations are integrated on Lagrangian grid by explicit methods: OD term – by one-step method, the others – by Lax–Wendroff method. Model properties (Table 1) are derived from observed values: column density, radius and line of sight magnetic field [7].

2.3 2D model features

Equation (1) is transformed to

$$\frac{\partial \vec{B}}{\partial t} = \nabla \times \left(\vec{v}_n \times \vec{B} + u\vec{B} - \eta_* \nabla \times \vec{B} \right), \tag{2}$$

Table 1 The properties of 1D models: core mass M, initial radius R_0, temperature T, central density n_{c0}, magnetic induction B_{c0}, the ratios of thermal and magnetic energies to the absolute value of gravitational energy, ε_t, ε_m.

Model	$M/M_\odot$	R_0, pc	n_{c0}, cm^{-3}	T, K	B_{c0}, mG	ε_t	ε_m
W3(main)	37	0.12	5.0e5	60	0.58	0.22	0.33
NGC 2024	10	0.20	5.5e5	25	0.12	0.39	0.06
DR21 OH 1	8	0.05	5.5e6	50	1.00	0.31	0.16

where $u = (4\pi R_{pn})^{-1}\,\vec{B}\cdot\left(\nabla\times\vec{B}\right)$ is the scalar velocity of AD, $\eta_* = \eta + (4\pi R_{pn})^{-1}\,B^2$ is the total coefficient of OD and AD. Density and velocity are axially symmetric; cylindrical coordinates are used. Energy equation includes the heating by CR and photoeffect, the cooling in molecular lines, and gas-grains collisions. The dust absorbtion of heating radiation from stars is calculated by the method of short characteristics. MHD equations are integrated on adaptive grid with the help of numerical code Enlil: hyperbolic terms – by HLLD method [8], the parabolic terms – by an implicit method. Initially $\rho(r)$ is constant that equals the external value from 1D model; $B(r)$ is constant that is fitted to pass the initial central (ρ, B) point of 1D model. Cloud mass is the same as in 1D model. The ratio of rotational energy to the absolute value of gravitational energy equals 0.001.

3 Results

1D models run up to protostellar densities ($n \gtrsim 10^{18}$ cm^{-3}). The number density ratio of electrons and neutrals x_e (the main factor of σ) is minimal in the region with $T \approx 1000$ K located at 0.5–5 AU (Fig. 1, left). Here OD is maximal while AD is weak due to the friction between charged grains and neutrals. Strong OD leads to the local minimum or plateau of $B(r)$ at $1-100$ AU (Fig. 1, right). At $T = 2300$ K grains disappear and AD becomes dominating, however this transition is not important for magnetic field evolution because magnetic Reynolds number $R_m \gg 1$ here.

Figure 1 (right) shows that $B(r)$ distribution in 1D model NGC 2024 is close to observed points (r, B) both for classical T Tauri stars and FU Orionis disk. However an exact fit to observational data is impossible in 1D models because there is no a plateau on $B(r)$ curve near kilo-gauss level. We speculate that this plateau can appear in 2D models if B_{ad} is amplified by the disk rotation.

Our 2D models of W3(main), NGC 2024 and DR21 OH 1 simulate only initial collapse stage because of insufficient spatial resolution. Magnetically and thermally supported disk (Fig. 2) forms in all the models, and so the density gradient along rotational axis becomes very large. Nevertheless 2D models show that 1D models overestimate the magnetic field at initial collapse stage (see Fig. 3, left).

Figure 3 (right) shows for 1D models the radial distributions of dimensionless number $A \equiv v_a^2/(\eta\Omega)$, where v_a is Alfven speed, Ω is the Keplerian rotation frequency. Magnetorotational instability is unable to generate MHD turbulence if $A < 1$ (dead zone) [9]. The dead zones are located at 0.5–30 AU where x_e is low. We find that

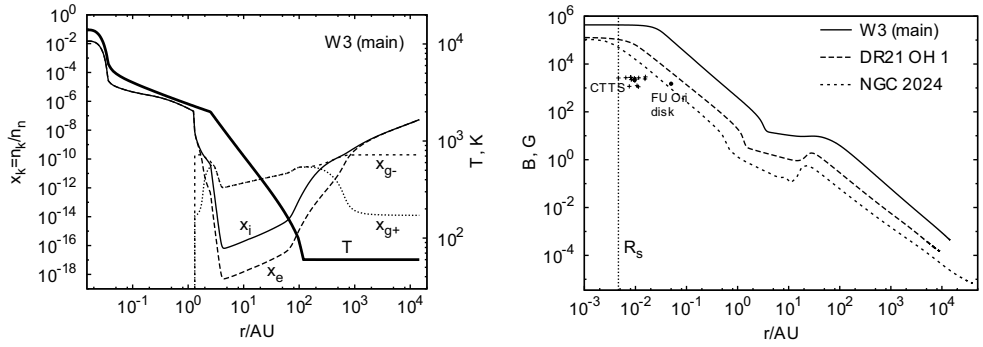


Figure 1 The radial distributions in 1D models: left – kinetic temperature and number density ratios of charged particles and neutrals; right – magnetic field intensity. The observed points (r, B) for classical T Tauri stars (crosses) and FU Orionis disk (circle) are shown also at right panel.

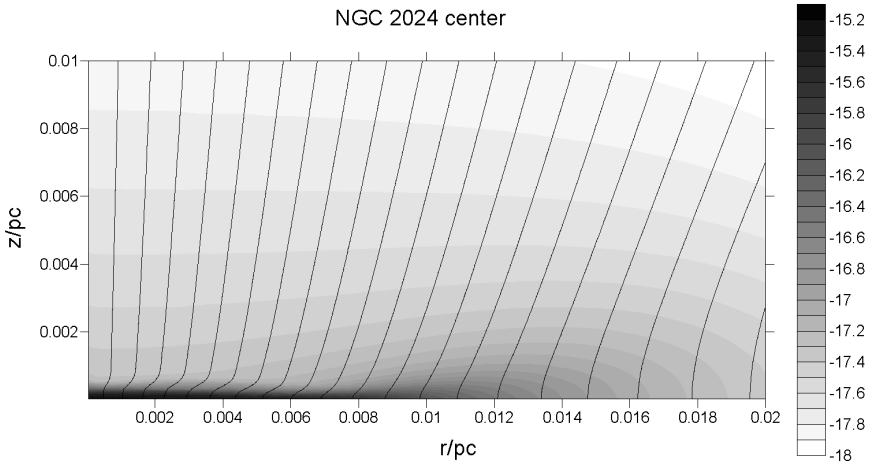


Figure 2 Distributions of density (logarithmic gray scale) and the root of magnetic flux (lines) at the central region of 2D model NGC 2024.

dead zone becomes nearer to a star if initial magneto-hydrostatic configuration has denser envelope due to the higher values of temperature and/or magnetic induction.

4 Conclusions

Using a self-similar solution for prestellar core collapse Krasnopolsky and Konigl [10] concluded that protostellar accretion disk is magneto-rotationally stable because of strong AD. However this solution is obtained at the cost of unreliable assumptions such as $T = const$, $n_i \propto n_n^{1/2}$, $v_a = const$, the cloud is a thin disk with central point mass, there is no OD, etc. Our 1D models dispense with these assumptions but use the approximation of centrally symmetric contraction. It causes two effect: a) the

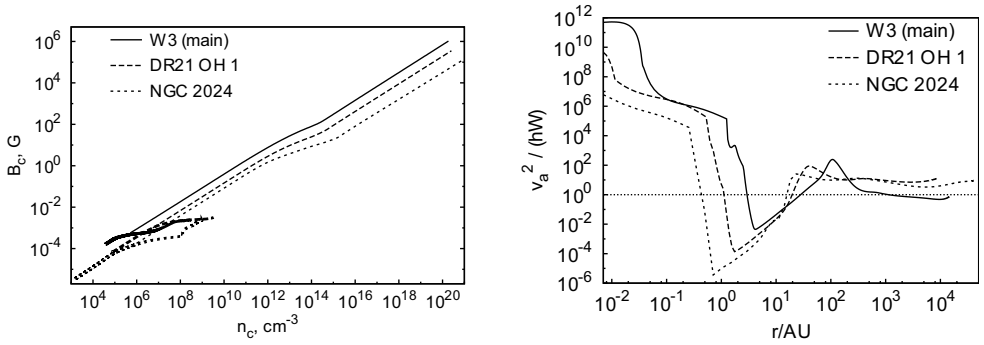


Figure 3 Left – magnetic field versus density in the center of 1D models (thin lines) and 2D models (thick lines). Right – the radial distributions of dimensionless number $A \equiv v_a^2/(\eta\Omega)$ in 1D models. MHD turbulence is not generated by magnetorotational instability if $A < 1$ (dead zone) [9].

overestimation of v_a and more narrow dead zones, b) the shift of x_e minimums and dead zones to a star.

2D models can give more realistic predictions of $\vec{B}_{\rm ad}$ and dead zone location. To achieve the protostellar densities in 2D models we plan the following steps: 1) the parallelization of code Enlil, 2) the use of initial magneto-hydrostatic configuration to prevent strong shocks, 3) the adaptation of radiative transfer solver to optically thick regime.

Acknowledgements

The work is supported by grant RFBR 07-02-96028-p2004 Ural. We wish to acknowledge A.E. Dudorov for useful criticism.

References

[1] Machida M.N., Tomisaka K., Matsumoto T., Inutsuka S. 2008, ApJ, 677, 327
[2] Donati J.F., Jardine M.M., Gregory S.G., Bouvier J., Dougados C., Menard F. 2008, arXiv:0804.0683
[3] Gammie C.F. 1996, ApJ, 457, 355
[4] Tassis K., Mouschovias T.Ch. 2007, ApJ, 660, 370
[5] Tassis K., Mouschovias T.Ch. 2005, ApJ, 618, 769
[6] Masunaga H., Inutsuka S. 2000, ApJ, 531, 350
[7] Crutcher R.M. 1999, ApJ, 520, 706
[8] Miyoshi T., Kusano K. 2005, JCoPh, 208, 315
[9] Sano T., Inutsuka S. 2001, ApJ, 561, L179
[10] Krasnopolsky R., Konigl A. 2002, ApJ, 580, 987